

NJC

New Journal of Chemistry

Accepted Manuscript

A journal for new directions in chemistry

This article can be cited before page numbers have been issued, to do this please use: H. Fang, Y. Chen, X. Shi, B. Yang, Z. Chen, Z. Han, Y. Zhang, W. He and Z. Guo, *New J. Chem.*, 2019, DOI: 10.1039/C9NJ03846A.



This is an Accepted Manuscript, which has been through the Royal Society of Chemistry peer review process and has been accepted for publication.

Accepted Manuscripts are published online shortly after acceptance, before technical editing, formatting and proof reading. Using this free service, authors can make their results available to the community, in citable form, before we publish the edited article. We will replace this Accepted Manuscript with the edited and formatted Advance Article as soon as it is available.

You can find more information about Accepted Manuscripts in the [Information for Authors](#).

Please note that technical editing may introduce minor changes to the text and/or graphics, which may alter content. The journal's standard [Terms & Conditions](#) and the [Ethical guidelines](#) still apply. In no event shall the Royal Society of Chemistry be held responsible for any errors or omissions in this Accepted Manuscript or any consequences arising from the use of any information it contains.

ARTICLE

Tuning lipophilicity for optimizing H₂S sensing performance of coumarin-merocyanine derivatives

Hongbao Fang, Yuncong Chen*, Xiangchao Shi, Yang Bai, Zhongyan Chen, Zhong Han, Yuming Zhang, Weijiang He* and Zijian Guo

Received 00th January 20xx,
Accepted 00th January 20xx

DOI: 10.1039/x0xx00000x

Hydrogen sulfide (H₂S) is an endogenous signaling molecule involving with various physiopathological process, coumarin-based merocyanines have been successfully utilized for developing fluorescent H₂S sensors. However, subtle changes on the chemical structure of merocyanines could induce distinct difference in H₂S sensing behavior. Investigation on the structure-property relationship of merocyanine dyes is of great importance for the development of ideal sensors with desirable performance. In this work, a series of coumarin/merocyanine (**CMC**) hybrid fluorescent probes with different lipophilicities have been developed. By altering the N-alkyl chain, the reaction rate with H₂S and intracellular distribution of **CMC** sensors are optimized. The results showed that increasing lipophilicity by attaching longer N-alkyl chain leads to faster sensing response as well as higher efficiency of mitochondrial targeting ability. By virtue of rapidly sensing of H₂S and impressive mitochondrial co-localization ability, **CM-NC₆** could monitor H₂S level via a dual channel ratiometric mode. In addition, **CM-NC₆** is also capable of *in vivo* imaging of exogenous H₂S. The work provided a powerful strategy for developing H₂S sensors with optimized performance, which would be helpful for understanding the complicated roles of H₂S in various physiological processes.

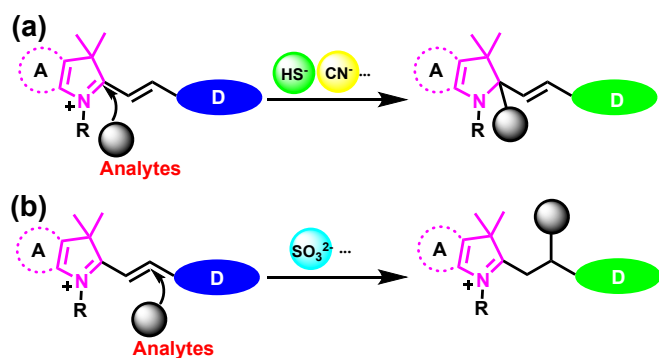
Introduction

Fluorescence imaging has evolved as one of the most reliable techniques to offer spatial-temporal information, which has displayed numbers of virtues including quick response, high sensitivity and non-invasiveness.¹⁻³ Near infrared (NIR) dyes show excellent photochemical properties, such as deeper penetration depth and minimum background auto-fluorescence, which are favorable for fluorescence imaging *in vivo*. Merocyanine dyes as a classic type of NIR molecules containing a D-π-A structure, exhibit long and strong absorption band attributed to the intramolecular charge transfer (ICT) process within the skeleton.⁴⁻⁶ Moreover, merocyanine molecules are endowed with the ability to target mitochondria due to its lipophilic cationic feature.^{5, 7} Therefore, merocyanine dyes are widely used for fluorescence sensing and bio-imaging. Due to the electron deficiency of the indolium part, nucleophilic addition was adopted as a powerful strategy for chemo-sensing. As depicted in **Scheme 1**, the nucleophilic addition reaction of the analytes to merocyanine dyes caused the break of the skeleton and the ICT process, resulting large alterations in both absorption and emission spectra.^{5a, 8}

Based on the nucleophilic addition mechanism, many merocyanine dyes have been reported to detect various species, such as HS⁻, CN⁻, SO₃²⁻ and so on (**Scheme S1**).⁸⁻¹⁰ We developed a coumarin/merocyanine hybrid fluorescent probe (**CouMC**) for H₂S detection, which showed the quick ratiometric H₂S sensing speed and the impressive mitochondria targeting ability.⁴ Kim and his colleagues invented a coumarin derivative for KCN detection, which showed blue-shift absorption spectra and turn-on emission spectra changes specially for KCN. Meanwhile theoretical calculations indicated that the increased fluorescence signal is caused by the prohibition of the ICT process.¹⁰ Chang and his colleagues reported a ratiometric probe **Mito-Ratio-SO₂** to detect mitochondrial SO₂ derivatives. Upon addition of sulphite, **Mito-Ratio-SO₂** exhibited a blue-shift dual emission spectra changes.^{5a} Comparing with these three probes, it could be concluded that subtle structural changes might lead to the distinct alteration of sensing behaviour. Particularly, coumarin/merocyanine hybrid fluorescent probes showed high specificity towards H₂S against other biological nucleophilic species (CN⁻ and SO₃²⁻). Therefore, understanding the structure-property relationship of merocyanine dyes is of great importance for developing sensors with desirable performance.

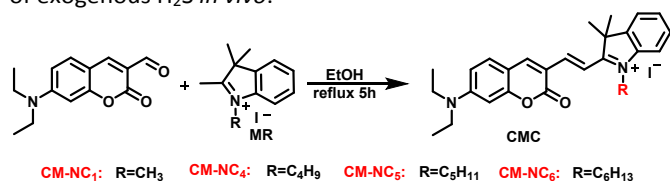
State Key Laboratory of Coordination Chemistry, School of Chemistry and Chemical Engineering, Nanjing University, Nanjing, 210023
Email: chenyc@nju.edu.cn; hewej69@nju.edu.cn

Electronic Supplementary Information (ESI) available: See DOI: 10.1039/x0xx00000x



Scheme 1 Mechanism schematic for the nucleophilic addition of merocyanine dyes. Nucleophilic addition reaction of the analytes to (a) the indolium C atom (named C-2) and (b) the C=C (named C-4) of the corresponding dyes.

Although widely known as a toxic gaseous molecule, H₂S has been regarded as the third signalling gas following by carbon monoxide and nitric oxide.¹¹ Many researches have reported that the disorder of H₂S level is closely associated with neurodegenerative disease, metabolic disease and even cancers.¹² Therefore, to develop efficient detection methods for H₂S *in vivo* has been of significance. Most reported probes for H₂S detection were based on a certain chemical reaction between H₂S and the probe with relatively slow response rate, which makes it difficult to offer the *in situ* and real time information of H₂S.¹³ It is challenging to construct fluorescent probes with quick response and ratiometric sensing ability to realize the intracellular or even subcellular H₂S imaging. In this regard, merocyanine dyes were especially appreciated for their superior capacity to monitor H₂S in mitochondria.^{14, 15} Herein, a series of coumarin/merocyanine hybrid fluorescent probes with different indole-*N*-alkyl group have been designed and synthesized (**Scheme 2**). The effect of lipophilicity on the sensing behaviour including response time and subcellular localization were systematically investigated. The results showed that the longer *N*-alkyl chain will lead to the faster sensing response to H₂S and more effective mitochondria targeting ability. **CM-NC₆** exhibit the best performance and was able to monitor intracellular H₂S fluctuation and imaging of exogenous H₂S *in vivo*.



Scheme 2 Synthesis procedure of CMC compounds.

Experimental

Materials and instruments. The reactive sulfur species and other tested anions stock solutions were prepared from NaHS, Na₂SO₄, Na₂SO₃, NaHSO₃, Na₂CO₃, NaCl, NaBr, NaI, [N(C₄H₉)₄]CN with deionized water. All solvents and chemical materials were commercial available and of analytic grade. Mitochondria tracker

dyes, Mitotracker Deep Red 633 were bought from Invitrogen. The NMR spectra characterations were performed on Bruker Ascend 400 or Bruker DRX-500 with TMS as the standard reference. HRMS (high resolution mass spectra) was completed using an Agilent 6540 Q-TOF mass spectrometer. The pH data were measured by a pH meter, Model PHS-3C. All the fluorescence spectra and absorption spectra were recorded on a FluoroMax-4 (Horiba) spectrofluorometer and Lambda 35 (PerkinElmer) absorption spectrometer. The absolute fluorescence quantum yields were determined by the integrating sphere (Costum-built by Labshere, coated by Spectronon, teflon cuvette) and calculated by Horiba software. All cell imaging was carried out via Zeiss LSM710. *In vivo* imaging experiments were conducted by PerkinElmer IVIS Lumina K.

General Methods

Cell culture and confocal imaging. MCF-7 cells were cultured with RPMI 1640 medium (Gibco) containing 10% FBS (Gibco) in a cell incubator with 5% CO₂ at 37 °C. And then MCF-7 cells were firstly cultured in the presence of 5 μM CM-NC₆ for 15 min. 200 μM NaHS was *in-situ* added to the medium and cell images were collected after incubation for another 30 min.

MCF-7 cells were incubated by **CM-NC₁**, **CM-NC₄**, **CM-NC₅** and **CM-NC₆** (5 μM, 15 min) and in turn by Mito-tracker Deep Red 633 (1 μM, 15 min). The fluorescence images in the green channel for **CM-NC₁**, **CM-NC₄**, **CM-NC₅** and **CM-NC₆** were obtained from 660 nm to 750 nm with 488 nm excitation, and the fluorescence images in the red channel for Mito-tracker Deep Red 633 were collected 665-750 nm emission band with 633 nm excitation.

Determination of octanol-water buffer partition coefficients. All samples were guaranteed to be in the same weight. Octanol-water buffer partition coefficients (log *P*) were measured according to a modified protocol.¹⁶ A 4 mL portion of 20 mM pH 7.4 PBS and 4 mL *n*-octanol were introduced to a 10 mL centrifuge tube and mixed to make sure equilibration of the PBS and octanol on a shaker for 24 h. Given samples were added to the tubes and vortexed for 3 min. After the vortex, the tubes were centrifuged for 5 min with the rotate speed at 3000 rpm. The lower, water layer was then separated and the amount of samples present were quantified by UV-vis absorbance. The log *P* value for each sample was then calculated from the partitioning between the water and octanol layers.

***In vivo* fluorescence imaging.** *In vivo* experimental approaches were carried out in accordance with Nanjing University ethical guidelines. The nude mice (female, 8 weeks) were provided by Nanjing Biomedical Research Institution of Nanjing University.

For exogenous H₂S imaging, hind legs of the nude mice were skin-pop (s.p.) injected with **CM-NC₆** (20 μM, 25 μL) and imaged with 10 min interval. The *in vivo* fluorescence images were collected with emission at 670 nm and excitation at 580 nm using an IVIS Lumina K system (PerkinElmer). Next, the left hind leg was given PBS buffer (20 mM, 50 μL) as the control group; the right hind leg was given NaHS (1 mM, 50 μL) as the experimental group, and then images were collected within 30 min.

General synthesis of compound CMC. The indole derivatives (**MR**) were synthesized according to the literature.¹⁷ **MR** (1.0 mmol) and 7-diethylaminocoumarin-3-aldehyde (**2**) (1.0 mmol) were refluxed for 5 h in 10 mL absolute ethanol under N₂ atmosphere. The reaction process was tracked by TLC until to the less mass reagent reacted completely. After the removal of the solvent by rotate evaporating, the obtained blue products were separated by silica column chromatography as eluent with CH₂Cl₂: CH₃OH, 50:1 to 10:1, and the corresponding **CMC** products were obtained.

Results and discussion

Synthesis and optical characterizations. The synthesis procedure of **CMC** compounds was outlined in **Scheme 2**. 7-diethylaminocoumarin-3-aldehyde and the **MR** were synthesized. And then the final **CMC** compounds were obtained by a facile one-pot reaction of 7-diethylaminocoumarin-3-aldehyde and **MR** in absolute ethanol. The ¹H NMR, ¹³C NMR, and HR-MS characterization of **CMC** were shown in the Supporting Information.

Spectroscopic response of CMC. Firstly, we examined the photophysical properties of compounds **CMC**. The absorption and emission spectra of **CMC** in 20 mM PBS buffer (pH 7.4, 2% DMSO, v/v) are shown in **Fig. 1** and **Table 1**. Fluorescence spectra of compounds **CMC** exhibited a strong merocyanine emission peak ranging from 580 to 750 nm (**Fig. 1a**), overlaying the NIR region (650–900 nm), which indicating that **CMC** possess the potential *in vivo* imaging. Meanwhile, almost no coumarin emission band at 500 nm was observed. The absolute fluorescence quantum yields of compounds **CMC** were also summarized in **Table 1**. The absorption spectra of **CMC** displayed a strong ICT band at about 570 nm with large molar absorption coefficients (>10⁴ M⁻¹cm⁻¹) (**Fig. 1b**). Given that merocyanine dyes can detect various species based on nucleophilic addition reaction, the selectivity of **CMC** was examined. However, the typical nucleophile SO₃²⁻, CN⁻ and other anions (Cl⁻, CO₃²⁻, Ac⁻, I⁻, HPO₄²⁻, Br⁻, P₂O₇²⁻, 1 mM), reactive sulfur species (HSO₃⁻, S₂O₃²⁻, 1 mM) led to almost minor change of the ratio, as shown in **Fig. 2**. Interestingly, only HS⁻ induce an obvious enhancement of the ratio F₄₉₃/F₆₄₅, which fully demonstrated that **CMC** probes were highly selective to HS⁻.

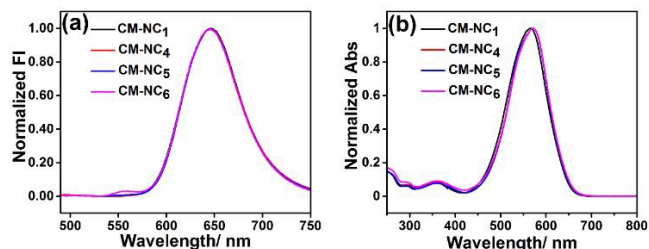


Fig. 1 Normalized emission (a) and absorption spectra (b) of **CMC** compounds in 20 mM PBS. $\lambda_{\text{ex}}=475$ nm.

Table 1. Photophysical properties of **CMC** in 20 mM PBS.

Compounds	$\lambda_{\text{abs}}^{(a)}/\text{nm}$	$\epsilon_{\text{max}}/10^4 \text{ M}^{-1}\text{cm}^{-1}$	$\lambda_{\text{em}}^{(b)}/\text{nm}$	$\Phi_f^{(c)}/\%$
-----------	--	---	---------------------------------------	-------------------

CM-NC₁	565	6.25	647	4.96
CM-NC₄	571	6.91	647	3.42
CM-NC₅	571	6.26	647	5.89
CM-NC₆	572	6.76	647	4.23

(a) The maximum absorption wavelength of the compounds. (b) The maximum emission wavelength of the compounds. (c) Φ_f measured using integrating sphere. The QYs are corresponding to maximum emission peaks.

Next, we examined the response time of **CMC** toward H₂S. As expected, when NaHS was dropped into the **CMC** solution, the fluorescence signal at 645 nm decreased, due to HS⁻ nucleophilic addition to indolenium C-2 atom of **CMC** at different response rate, as shown in **Fig. S1a-d**. As demonstrated in **Fig. 3a**, fluorescence intensity changes of **CMC** (10 μM) with NaHS (200 μM) addition indicated that the response could be finished by the extent with 65.1% in 16 minutes (**CM-NC₁**), 88.3% in 10 minutes (**CM-NC₄**), 93.6% in 4 minutes (**CM-NC₅**) and 97.8% in 40 seconds (**CM-NC₆**), respectively. The similar phenomenon was observed through absorption changes with 20 equiv. NaHS to the **CMC** solution (**Fig. 3b** and **Fig. S2a-d**). The results demonstrated that longer N-alkyl chain led to the faster sensing response to H₂S.

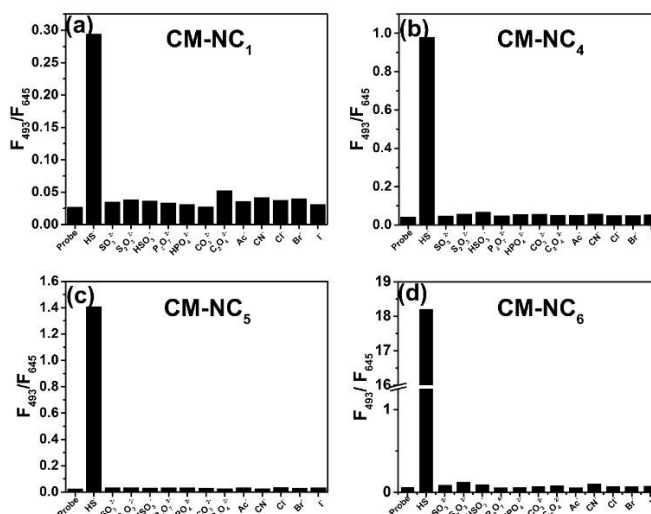


Fig. 2 F_{493}/F_{645} of 10 μM **CMC** (10 μM) in 20 mM PBS treated with HS⁻ (200 μM) or various other anions (1 mM). $\lambda_{\text{ex}}=475$ nm.

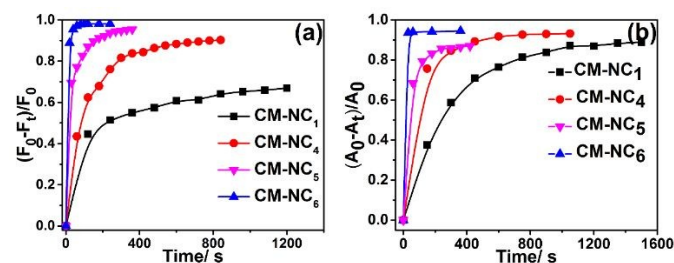


Fig. 3 (a) Fluorescence intensity changes (F_0-F_t)/ F_0 of **CMC** (10 μM) with 200 μM NaHS, $\lambda_{\text{ex}}=475$ nm. (b) absorption changes (A_0-A_t)/ A_0 of **CMC** (20 μM) with 400 μM NaHS.

Owing to its fast response to H₂S, **CM-NC₆** turns into the best choice to make further investigation. Upon the NaHS (0-100 μM) titration to **CM-NC₆** solution, the conjugation of merocyanine molecule was destroyed, resulting in its coumarin emission band 495 nm undergoing a distinct enhancement, while the merocyanine band at 645 nm decreasing simultaneously (Fig. 4a). The emission ratio (F₄₉₃/F₆₄₅) increased from 0.038 to 18.2 by 478-fold. And the detection limit was measured as 0.49 μM (Fig. S3). The similar phenomenon was observed via the absorption spectra (Fig. 4b). With the introduction of HS⁻, the ICT band at 572 nm gradually dropped, indicating HS⁻ broke the ICT effect in the merocyanine molecule. In addition, we observed that the dark blue **CM-NC₆** solution turned to pale yellow following with added 20 equiv. NaHS, which means **CM-NC₆** achieved the detection visualization of HS⁻.

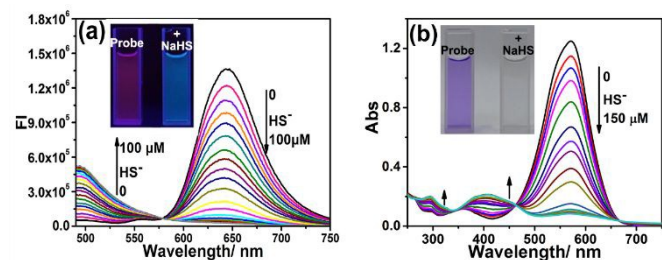


Fig. 4 (a) Fluorescence titration of 10 μM **CM-NC₆** in PBS with the concentration of HS⁻ (0-100 μM), λ_{ex}= 475 nm; (b) Absorption titration of 20 μM **CM-NC₆** in PBS with the concentration of HS⁻ (0-150 μM). Inset in (a): fluorescence photo of **CM-NC₆** irradiated by a 365 nm lamp without or with of HS⁻. Inset in (b): natural photo of **CM-NC₆** without or with HS⁻.

HS⁻ sensing competition experiments of **CM-NC₆** in the presence of other biothiols was also investigated. Only a minor change of emission ratio were induced by GSH, Cys or Hcy (Fig. 5a). The HS⁻ sensing competition behaviour demonstrated that **CM-NC₆** is capable to sense HS⁻ without any interference with GSH, Cys or Hcy. The pH-dependence of **CM-NC₆** was evaluated (Fig. 5b) as well. The emission ratio of **CM-NC₆** displayed little variation in the pH (2.3-8.0), implying that **CM-NC₆** is stable in physiological pH range. It provided an important basis for the detection of H₂S in physiological environment.

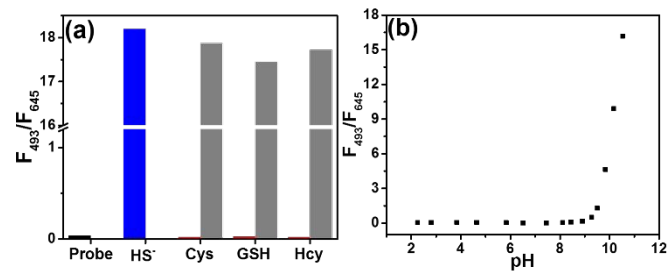


Fig. 5 (a) F₄₉₃/F₆₄₅ of **CM-NC₆** (10 μM) in PBS buffer with 200 μM HS⁻, 1 mM GSH, 1 mM Cys, and 200 μM Hcy. (a): black bar represents **CM-NC₆**, or blue bar represents **CM-NC₆** with HS⁻ or black bar represents **CM-NC₆** with common biotriols, gray bars represent **CM-NC₆** in the presence of common biotriols followed by adding with HS⁻ (200 μM). (b) F₄₉₃/F₆₄₅ of 10 μM **CM-NC₆** at different pH value. λ_{ex}= 475 nm.

Colocalization imaging of CMC in living cells. Cellular distribution of CMC was studied using a confocal microscopy in MCF-7 cells. Owing to the indolium part with the positive charge, the probes can effectively locate in mitochondria.¹⁸

The green channel images for **CMC** were obtained with 488 nm excitation and the red channel images for the Mito-Tracker were collected with 633 nm excitation (Fig. 6). The Pearson's correlation coefficient (PCC) of **CM-NC₁** calculated by Zeiss software is only 0.67. However, when indole-N-alkyl chain gets longer, the PCC gets higher, 0.88 for **CM-NC₄**, 0.90 for **CM-NC₅** and 0.91 for **CM-NC₆**, respectively. It indicated that the probe with shorter indole-N-alkyl chain is less lipophilic and more difficult to pass through the mitochondrial membrane.¹⁹ Therefore, **CM-NC₁** possesses poorer target-mitochondria ability, when indole-N-alkyl chain length achieve above C₄ (**CM-NC₄**, **CM-NC₅** or **CM-NC₆**), lipophilicity enhancement benefit probes to target mitochondria.

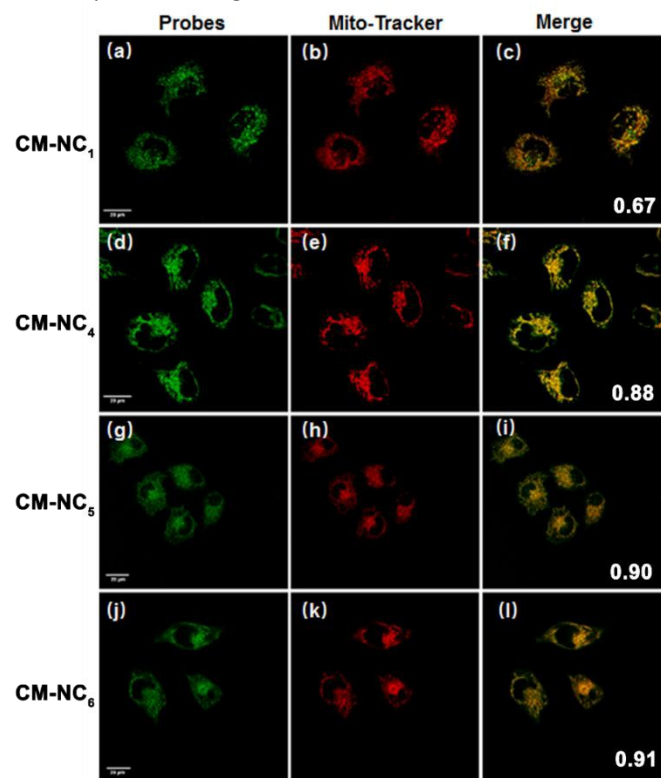


Fig. 6 Confocal images of MCF-7 cells incubated with **CMC** (5 μM, 15 min) and Mitotracker Deep Red 633 (1 μM, 15 min). (a,d,g,j) The green channel images of **CMC** with 488 nm excitation; (b,e,h,k) The red channel images of Mitotracker Deep Red 633 with 633 nm excitation; (c,f,i,l) overlay of (a,d,g,j) and (b,e,h,k). Scale bar = 20 μm.

Table 2. Lipophilicity, charge of **CMC** in solution and mitochondrial PCC of **CMC** in MCF-7 cells.

Compounds	LogP ^(a)	Charge ^(b)	Mitochondrial PCC
CM-NC₁	0.590	+	0.67
CM-NC₄	2.391	+	0.88
CM-NC₅	3.690	+	0.90
CM-NC₆	3.842	+	0.91

(a) The values of Log P were determined in octanol/ PBS (20 mM, pH7.4) by an improved procedure. (b) Charge of **CMC** in PBS.

The log P of **CMC** were measured to investigate the relationship of lipophilicity with mitochondrial colocalization behaviour.^{20, 21} We then listed the log P, charge of **CMC** in PBS (20 mM, pH7.4), and mitochondrial PCC (Table 2). Based on these data, we concluded that **CMC** with cationic charge alone is insufficient to ensure mitochondria targeting, higher lipophilicity is another requirement for effective mitochondrial targeting.

Fluorescence imaging of CM-NC₆ in MCF-7 cells. The intracellular H₂S imaging of **CM-NC₆** was investigated in MCF-7. The cells loaded with 5 μM **CM-NC₆** for 15 min displayed weak fluorescence in the green channel and strong fluorescence signal in the red channel, indicating the good cell-permeability of **CM-NC₆**. The dim ratiometric image (green/red) was obtained. Interestingly, incubation with 200 μM NaHS led to a faint enhancement in green channel, at the same time the red channel fluorescence signal obviously dropped, and the ratiometric image displayed a distinct change, as shown in Fig. 7. It is demonstrated that **CM-NC₆** can detect the intracellular exogenous H₂S via a dual channel ratiometric mode, and the related ratio enhancement factor can reach up to 5-fold.

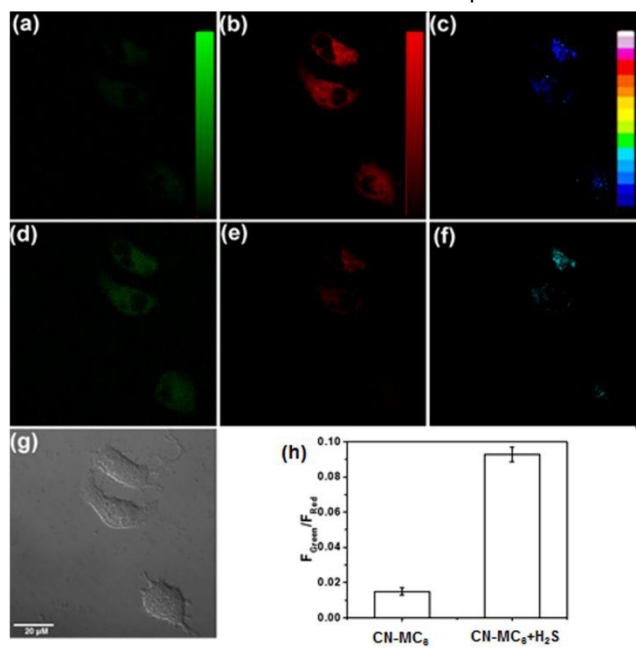


Fig. 7 Confocal images of MCF-7 cells with 488 nm excitation. (a-c) confocal images of MCF-7 cells loaded with **CM-NC₆** (5 μM, 15 min); (d-f) confocal images of loaded-**CM-NC₆** (5 μM, 15 min) MCF-7 cells in-situ added with 200 μM NaHS for 30 min. (c, f) ratiometric confocal images acquired by green channels (a, d) from 500-580 nm and the corresponding red channels (b, e) from 632-700 nm; (g) Bright-field image of MCF-7 cells; (h) Average intensity ratio values ($F_{\text{Green}}/F_{\text{Red}}$) of (c) and (f). Scale bar = 20 μm.

In vivo fluorescence imaging of CM-NC₆ in mice. Prominent features were showed by **CM-NC₆**, such as NIR emission, rapid response, high specificity and excellent biocompatibility. These appropriate characteristics inspired us to further explore the potential of **CM-NC₆** for visualizing H₂S *in vivo*. We first examined the feasibility of **CM-NC₆** for detecting exogenous H₂S in mice. Mice were skin-pop injected with **CM-NC₆** and NaHS, and then imaged using IVIS imaging system with excitation at 580 nm and emission at 670 nm. **CM-NC₆** was injected to the legs (20 μM, 25 μL) after the mice were

anesthetized. After that, the left leg was given PBS buffer (20 mM, 50 μL) as the control group; the right leg was given NaHS (1 mM, 50 μL) as the experimental group. As seen in Fig. 8b, the leg injected with NaHS exhibited a much lower fluorescence intensity than the leg injected with PBS. We measured the fluorescence signal intensity collected from the legs in the mice by *in vivo* system software, as displayed in Fig. 8c, the readout data indicated that the exogenous H₂S could lead to approximately 1-fold lower fluorescence intensity than the control leg with PBS treatment. Thus, the above results indicated that **CM-NC₆** are capable to be apply for imaging H₂S *in vivo*.

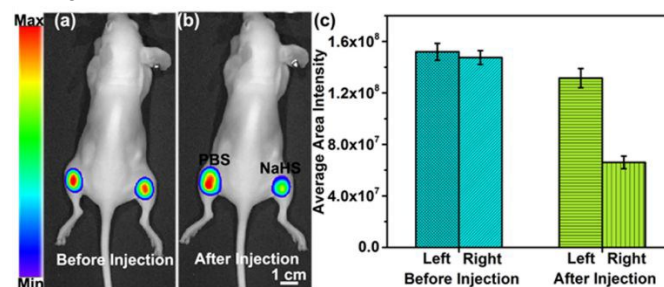


Fig. 8 *In vivo* fluorescence imaging of exogenous H₂S in mice. (a) Only s.p. injected with **CM-NC₆**; (b) Then s.p. injected with PBS (left leg) and NaHS (right leg). (c) Values of emission intensity from the leg area of (a) and (b).

Conclusions

In summary, a series of coumarin/merocyanine hybrid fluorophores with different indole-N-alkyl groups were prepared. Spectroscopic study disclosed that **CM-NC₁**, **CM-NC₄**, **CM-NC₅**, and **CM-NC₆** all display the excellent ratiometric sensing ability specifically for H₂S in aqueous medium, which is not interfered by the normal anions and nucleophiles in living systems, such as Cys, GSH and Hcy. Moreover, the higher lipophilicity (longer N-alkyl chain) leads to the faster sensing response to H₂S. Among these probes, **CM-NC₆** with N-hexyl group demonstrated the fastest response time within 40 s. The mitochondria co-localization indicated that the mitochondria targeting ability was also relative with the lipophilicity of the compounds. **CM-NC₆** was able to sense the intracellular H₂S deviation triggered by the exogenous H₂S addition via a dual channel ratiometric mode. **CM-NC₆** also can be used for *in vivo* imaging of exogenous H₂S without autofluorescence. We are confident that this design tactic could be applied for construction of H₂S probes with faster response and more effective organelle-targeted ability in the future, which would be beneficial for the study of various H₂S functions in physiological processes.

Conflicts of interest

This work is patent pending by the State Intellectual Property Office of P. R. C., and the patent pending number is 201810881196.8.

Ethical statement

All animal procedures were performed in accordance with the Guidelines for Care and Use of Laboratory Animals of Nanjing University and experiments were approved by the Animal Ethics Committee of Nanjing University

Acknowledgements

We are grateful to the financial supports from the National Natural Science Foundation of China (Grants 21571099, 21731004), the National Basic Research Program of China (Grant 2015CB856300), the Natural Science Foundation of Jiangsu Province (BK20150054) and the Fundamental Research Funds for the Central Universities (020514380172).

Notes and references

- (a) A. R. Lippert, E. J. New, C. J. Chang, *J. Am. Chem. Soc.*, 2011, **133**, 10078; (b) H. Peng, Y. Cheng, C. Dai, A. L. King, B. L. Predmore, D. J. Lefer, B. Wang, *Angew. Chem. Int. Ed.*, 2011, **50**, 9672.
- (a) F. Yu, X. Han, L. Chen, *Chem. Commun.*, 2014, **50**, 12234.
- (a) X. Wang, J. Sun, W. Zhang, X. Ma, J. Lv, B. Tang, *Chem. Sci.*, 2013, **4**, 2551; (b) G. Li, S. Ma, J. Tang, Y. Ye, *New J. Chem.*, 2019, **43**, 1267; (c) C. Zhang, L. Wei, C. Wei, J. Zhang, R. Wang, Z. Xi, L. Yi, *Chem. Commun.*, 2015, **51**, 7505; (d) L. Zhang, X. E. Zheng, F. Zou, Y. Shang, W. Meng, E. Lai, Z. Xu, Y. Liu, J. Zhao, *Sci. Rep.*, 2016, **6**, 18868.
- Y. Chen, C. Zhu, Z. Yang, J. Chen, Y. He, Y. Jiao, W. He, L. Qiu, J. Cen, Z. Guo, *Angew. Chem. Int. Ed.*, 2013, **52**, 1688.
- (a) W. Xu, C. L. Teoh, J. Peng, D. Su, L. Yuan, Y. Chang, *Biomaterials*, 2015, **56**, 1; (b) J. Xu, H. Yuan, C. Qin, L. Zeng, G. Bao, *RSC Adv.*, 2016, **6**, 107525; (c) S. Samanta, S. Halder, P. Dey, U. Manna, A. Ramesh, G. Das, *Analyst*, 2018, **143**, 250.
- (a) X. Huang, X. Gu, G. Zhang, D. Zhang, *Chem. Commun.*, 2012, **48**, 12195; (b) Y. Yue, F. Huo, S. Lee, C. Yin, J. Yoon, J. Chao, Y. Zhang, F. Cheng, *Chem. Eur. J.*, 2016, **22**, 1239.
- Y. Chen, C. Zhu, J. Cen, Y. Bai, W. He, Z. Guo, *Chem. Sci.*, 2015, **6**, 3187.
- (a) L. He, X. Yang, K. Xu, X. Kong, W. Lin, *Chem. Sci.*, 2017, **8**, 6257; (b) C. Yin, F. Huo, M. Xu, C. L. Barnes, T. E. Glass, *Sensor Actuat B-Chem*, 2017, **252**, 592.
- (a) G. Song, J. Luo, X. Xing, H. Ma, D. Yang, X. Cao, Y. Ge, B. Zhao, *New J. Chem.*, 2018, **42**, 3063; (b) J. Yang, K. Li, J. Hou, L. Li, C. Lu, Y. Xie, X. Wang, X. Yu, *ACS Sens.*, 2015, **1**, 166.
- H. J. Kim, K. C. Ko, J. H. Lee, J. Y. Lee, J. S. Kim, *Chem. Commun.*, 2011, **47**, 2886.
- V. S. Lin, W. Chen, M. Xian, C. J. Chang, *Chem. Soc. Rev.*, 2015, **44**, 4596.
- S. Fiorucci, E. Antonelli, A. Mencarelli, S. Orlandi, B. Renga, G. Rizzo, E. Distrutti, V. Shah, A. Morelli, *Hepatology*, 2005, **42**, 539.
- (a) J. Chen, M. Zhao, X. Jiang, A. Sizovs, M. C. Wang, C. R. Provost, J. Huang, J. Wang, *Analyst*, 2016, **141**, 1209; (b) S. Wang, S. Xu, G. Hu, X. Bai, T. D. James, L. Wang, *Anal. Chem.*, 2016, **88**, 1434; (c) T. Liu, Z. Xu, D. R. Spring, J. Cui, *Org. Lett.* 2013, **15**, 2310; (d) L. A. Montoya, M. D. Pluth, *Chem. Commun.*, 2012, **48**, 4767.
- J. W. Elrod, J. W. Calvert, J. Morrison, J. E. Doeller, D. W. Kraus, L. Tao, X. Jiao, R. Scalia, L. Kiss, C. Szabo, H. Kimura, C. Chow, D. J. Lefer, *P. Natl. Acad. Sci. USA*, 2007, **104**, 15560.
- C. Szabo, C. Ransy, K. Módis, M. Andriamihaja, B. Murghes, C. Coletta, G. Olah, K. Yanagi, F. Bouillaud, *Brit. J. Pharmacol.*, 2014, **171**, 2099.
- OECD Guideline for the Testing of Chemicals. Partition Coefficient (n-octanol/water): Shake Flask Method. ©OECD, 1995, 107.
- A. C. Pardal, S. S. Ramos, P. F. Santos, L. V. Reis, P. Almeida, *Molecules*, 2002, **7**, 320.
- (a) H. Zhu, J. Fan, J. Du, X. Peng, *Acc. Chem. Res.*, 2016, **49**, 2115; (b) J. Zielonka, J. Joseph, A. Sikora, M. Hardy, O. Ouari, J. Vasquez-Vivar, G. Cheng, M. Lopez, B. Kalyanaraman, *Chem. Rev.*, 2017, **117**, 10043; (c) K. Yang, J. L. Kolanowski, E. J. New, *Interface Focus*, 2017, **7**, 20160105.
- L. F. Yousif, K. M. Stewart, S. O. Kelley, T. *ChemBioChem*, 2009, **10**, 1939.
- R. W. Horobin, J. C. Stockert, F. Rashid-Doubell, *Histochem. Cell Biol.*, 2006, **126**, 165.
- W. Chyan, D. Y. Zhang, S. J. Lippard, R. J. Radford, *Proc. Natl. Acad. Sci. USA*, 2014, **111**, 143.

Published on 27 August 2019. Downloaded by Kings College London on 08/27/2019 22:53:37.
 See Article Online for Journal Details.
 DOI: 10.1039/C9NJ03640A